R. & M. No. 3170
(19,614)
A.R.C. Technical Report

MINISTRY OF AVIATION

AERONAUTICAL RESEARCH COUNCIL
REPORTS AND MEMORANDA

The Measurement of Unsteady Forces and Moments on Slender Bodies Oscillating in a Wind Tunnel

By

J. F. CLARKE, Ph.D.

LONDON: HER MAJESTY'S STATIONERY OFFICE
1960
EIGHT SHILLINGS NET

The Measurement of Unsteady Forces and Moments on Slender Bodies Oscillating in a Wind Tunnel

By

J. F. CLARKE, Ph.D.

Reports and Memoranda No. 3170

October, 1957

Summary.—An apparatus for the measurement of unsteady aerodynamic reactions on slender bodies is described. It is particularly suited to tests at supersonic speeds. The forces and moments on the model are detected by strain-gauges attached to the model mounting sting and by supplying their bridge circuits with properly phased A.C. of the right frequency, direct meter readings of the stiffness or damping reactions may be obtained.

The results of a short series of tests on a cone-cylinder at subsonic Mach numbers and reduced frequency parameters (based on model length) up to 0·06 are given.

1. *Introduction.*—Established techniques for the measurement of oscillatory aerodynamic forces in the wind tunnel suffer from several disadvantages when the model to be tested is a slender body of revolution and these are aggravated when the free-stream speeds required are high. The most serious of the problems encountered is that of support interference, particularly when the available wind tunnel is of small size.

It is virtually essential that such a model should be sting mounted and this creates some complications in the provision of a centre of rotation within the model's own length (other types of mounting, such as a spindle projecting from the tunnel side walls or a half-model technique plainly cannot compete with the sting mounting for bodies of such small lateral dimensions). With the sting mounting the forcing linkages, etc., are bound to be rather unwieldy and it is necessary to measure the reactions on the model alone, eliminating the friction and inertia of these linkages as far as possible.

The following describes an attempt to produce an apparatus which fulfils the general requirements outlined briefly above. At the time at which design work was commenced, information on unsteady force measurements, especially at high speeds, was rather scanty. A notable exception was the work of Bratt and Chinneck[1], on oscillating two-dimensional aerofoils, employing the classical logarithmic decrement method to measure damping and the change in natural frequency of vibration to measure stiffness. Otherwise, the free-stream speeds investigated were in the incompressible-fluid range and the work was mainly confined to two-dimensional aerofoils or whole aircraft models with a view to obtaining one derivative in particular from each piece of equipment. Techniques used in such tests may be found summarised in standard text books, *e.g.*, Piercy[2] or Duncan[3]. During the later stages of the development of the present equipment, a review of current methods in use at that time appeared (Valensi[4]) from which various advances in techniques were apparent, particularly in connection with force-sensing elements and the use of inexorable forcing systems in some cases. The present equipment contains some features which have not been described elsewhere to the writer's knowledge and it is therefore hoped that the following description will be of some interest.

The forcing system chosen was of the inexorable type, this being best suited to the sting mounting of the model. The actual design provided for an infinite choice of centre of rotation (when oscillating in a pitching mode) by changing the angles of the two driving swash plates.

Pure plunging motion could also be obtained if required. The amplitudes of these modes was also continuously variable by the same means, within upper limits set by the particular design. Frequency of oscillation was mainly limited by return-spring strength, but was also infinitely variable below this limit.

The aerodynamic reactions were measured by strain-gauges attached to the sting inside the hollow model. By supplying the strain-gauge bridge circuits with A.C. of the proper phase (relative to model displacement) and frequency (equal to that of the model's oscillations), it was possible to produce D.C. galvanometer readings directly proportional to the in-phase or out-of-phase reactions*. These included model inertia terms, which could easily be eliminated by consecutive wind-off, wind-on measurements.

2. *The Wind Tunnel.*—Before embarking on a description of the details of the apparatus it is necessary to describe briefly the essential features of the wind tunnel, as they exercised considerable influence on the final design.

It was of the closed return, intermittent type, operating on the injector principle, with alternative working-section dimensions of 5 in. by $5\frac{1}{2}$ in. or $3\frac{1}{2}$ in. by 8 in. Optically flat glass panels were situated in the two parallel walls of the working-section, the remaining pair of walls consisting of shaped wooden liners. Injector air was obtained from a storage vessel at a maximum pressure of 300 lb/in.^{2}, control to the injector box being through a manually operated valve. Running times were of the order of $1\frac{1}{2}$ to 2 minutes. Part of the working-section with the model and forcing gear in place can be seen in Fig. 1.

Model length was limited to about four inches to prevent interference by reflections from the tunnel side walls at a Mach number of 1·5 in the 5-in. by $5\frac{1}{2}$-in. section. To obtain frequency parameters of about 0·05 it was therefore necessary to arrange to oscillate the model at frequencies of about 20 c.p.s.

3. *The Apparatus.*—The apparatus consisted of two main units which were linked photoelectrically. Referring to Fig. 2, which is a block diagram of the equipment, these units were the mechanical forcing gear and the strain-gauge bridge circuits with their associated power supply and meters.

The photoelectric link consisted of an eccentric cam, mounted on the forcing-gear drive shaft, which interrupted a parallel beam of light falling on a photocell. The output of the latter was power amplified and fed to the bridge circuits, its phase relative to the model displacement being under control.

The various components will now be described in more detail.

3.1. *The Forcing Gear.*—Referring to Fig. 3, the model M was hollow and attached at A to the end of a sting S. S carried two pairs of strain gauges G (further details of which are given in Section 3.7), and was mounted on two horizontal supports, F and R. These had, respectively, a pivot point at P_1 and a sliding joint at P_2 and were constrained to move along horizontal paths by passing through the guide block B. B was rigidly attached to the wind-tunnel frame. F and R carried hemispherical hardened steel balls H in seatings in their outer ends. The flat faces of these balls were in contact with two swash plates, W_f and W_r, which were driven by an electric motor, T. The mechanical system was closed by the action of two coil springs in torsion, Ss (shown diagrammatically in Fig. 3).

Thus the model was caused to perform simple harmonic oscillations about any chosen point on the model's longitudinal axis. The motion induced in F or R by its swash plate is given by $x = r \tan\theta \sin \omega t$ when the latter rotates at constant angular speed ω. The distance between F (or R) and the swash-plate spindle centre-line is r and θ is the angle of the plate W_f (or W_r) to the axis of rotation.

* This method of measuring force components was first proposed by L. A. G. Sterne of the R.A.E. in 1951.

When the plates are ' in phase ' with one another, the motion imparted to the model is given by

$$\alpha = \tan^{-1}\{(r_r \tan\theta_r - r_f \tan\theta_f) \quad d^{-1} \quad \sin\omega t\}, \qquad \ldots \qquad \ldots \qquad \ldots \qquad (1)$$

α being the angular displacement of the model about point C (Fig. 4), and d the distance between F and R (suffixes refer to supports F or R). As an example, if the amplitude of α is 5 deg, about the maximum envisaged, and with values for d of 1·5 in., $r_r \tan\theta_r$ of 0·35 in. and $r_f \tan\theta_f$ of 0·22 in., expansion of equation (1) leads to

$$\alpha = 0{\cdot}0864 \sin\omega t + 0{\cdot}00005 \sin 3\omega t + \ldots\ldots$$

The harmonics introduced by making F and R move along rectilinear instead of circular paths can be seen to be of negligible size. The centre of oscillation C moves along the model axis during one cycle of the motion, but the amplitude of movement is very small, about 0·01 in., and can be ignored (it was reduced by making P_1 the pivot and P_2 the sliding joint).

The distances r_r and r_f were fixed, but it was possible to vary θ_r and θ_f at will, within upper limits set by the particular design, and by these means the amplitude of oscillation and centre of rotation could be varied. Variation of θ_f and θ_r, keeping the ratio $\tan\theta_f/\tan\theta_r$ constant, changed the amplitude while C remained fixed. If $\tan\theta_f/\tan\theta_r$ was changed the centre of rotation moved and when the ratio was 1 : 1, C was at infinity, *i.e.*, plunging motion. For the preliminary series of tests to be described here it was arbitrarily decided to construct a pair of swash plates to give a pitching amplitude of 3 deg about a point mid-way along the model.

The hemispheres in the support ends were necessary in order to maintain a constant distance between F and R and their swash-plate faces, thereby eliminating harmonics in the motion of the supports.

The shroud covering the supports for some distance into the working-section was found to be necessary in order to prevent excessive sideways twisting of the model and sting assembly. It can be seen in place in Fig. 1.

Fig. 3 is diagrammatic, a rather better idea of the lay-out of the forcing system being gained from the sketch, Fig. 5. Photographs of parts of the forcing gear are shown in Figs. 6 and 7 and the complete model mounting unit is shown in Fig. 8.

3.2. *The Sting.*—The sting (*see* Fig. 7) was carefully machined from Duralumin stock, the length which carried the strain-gauges having cross-sectional dimensions 0·20 in. deep by 0·15 in. wide. These dimensions were dictated more by model size than by considerations of sensitivity, but the latter proved to be adequate.

3.3. *Frequency Measurement.*—The frequency of oscillation of the model was measured with a revolutions counter (seen on the right of Fig. 1) and stopwatch. The revolutions counter could be zeroed and restarted while the electric motor was in motion.

3.4. *The Model.*—The model for this preliminary series of tests was a simple cone-cylinder of length 3·50 in. and diameter $\frac{3}{8}$ in. The cone semi-vertex angle was 8·5 deg and model thickness ratio was 10·7 per cent. It was made in two halves, so that the cylindrical portion could be tested with different nose shapes at a later stage, and also to facilitate manufacture. The material used was mild steel and machining was carried out to within 0·0005 in. of the nominal dimensions, particular attention being paid to the cone-cylinder junction. No disturbance of the airflow from this source was observed during the tests.

3.5. *The Measurement of Oscillatory Forces.*—The output from a strain-gauge bridge containing two active gauges (arranged to detect a moment applied to their support as an increase δr of resistance of one whilst the other undergoes a similar decrease of resistance) can be shown to be

$$i_3 = 2V\delta r\{P(R + 2r + r^2R^{-1}) + 2rR + 2r^2\}^{-1}$$

(The notation is explained in Fig. 9). This result is valid for both A.C. and D.C. energisation, provided the bridge impedances are of a purely resistive character.

Let it now be supposed that the moment producing the changes of resistance in the active gauges is time dependent. Then, if ω is the angular frequency of the fundamental mode of variation of the moment with time, we can write,

$$\delta r = a \sin \omega t + b \cos \omega t ,$$

plus a series of higher harmonics depending on the nature of the moment. Let it also be supposed that the voltage supply to the bridge is of the form $V = V_0 \sin \omega t$. Then the output from the bridge is proportional to

$$V \, \delta r = \frac{aV_0}{2} - \frac{V_0}{2} (a \cos 2\omega t - b \sin 2\omega t) .$$

It is observed that the output contains a D.C. component which is proportional to the product of the amplitude of the alternating supply voltage and the amplitude of that part of the moment in the sting which is in phase with the applied voltage. With the supply voltage phase shifted $\pi/2$, the relevant part of the output would be a function of b. Provided that the output can be smoothed sufficiently, a direct reading of in-phase and out-of-phase sting moments can then be made. Since it is an essential requirement that A.C. and D.C. bridge characteristics be identical, calibration can be effected statically, which is very convenient. Also, the system permits investigation of the static and dynamic aerodynamic characteristics of a particular model configuration together, by changing the supply voltage alone.

3.6. *Forces and Moments in the Sting.*—Fig. 4 shows the actual and effective (inertia) forces acting on the model. The former are the aerodynamic normal force and moment and axial force, denoted by N, M_a and X, and the reactions R_N, R_X and M_R, of the sting on the model. All of these are assumed to be acting at the centre of rotation C. The model's weight acts through G, the centre of gravity, distant l from C. The effective forces are F_N, F_X and M_I, all acting at G. The angular displacement of the model is given by $\alpha = \alpha_0 \sin \omega t$.

Equating actual and effective forces according to D'Alembert's principle gives

$$R_X + N + W \sin \alpha = F_N = \frac{W}{g} l\alpha_0 \omega^2 \sin \omega t ,$$

$$R_X + X + W \cos \alpha = F_X = - \frac{W}{g} l\alpha_0^2 \omega^2 \cos^2 \omega t ,$$

$$M_R + M_a + N \, . \, l + R_N \, . \, l = M_I = - \frac{W}{g} k^2 \alpha_0 \omega^2 \sin \omega t ,$$

where k is the radius of gyration of the model about G and g is the acceleration due to gravity. Thus we can find the moments in the sting at the strain-gauge measuring positions. Writing the distances between C and the effective gauge pair measuring positions as l_f and l_r for front and rear pairs respectively, these moments, M_f and M_r, are

$$M_{f,r} = (M_a + N \, . \, l_{f,r}) + (I_m - F \, . \, l \, . \, l_{f,r}) \sin \omega t - W(l - l_{f,r}) \sin \alpha ,$$

where $I_m = \alpha_0 \omega^2 (k^2 + l^2) W/g$ and $F = \alpha_0 \omega^2 \, . \, W/g$. The strain-gauges thus detect effects due to the aerodynamic reactions on the model, due to model inertia and model weight, but the latter two may be eliminated by making wind-on and wind-off measurements and need not be measured directly.

If the aerodynamic force and moment consist of parts in-phase and out-of-phase with α, *i.e.*, if we write

$$M_a = a \sin \omega t + b \cos \omega t$$

$$N = c \sin \omega t + d \cos \omega t ,$$

then the parts of $M_{f,r}$ due to the aerodynamic reactions are

$$M_{f,r} = (a + c \, . \, l_{f,r}) \sin \omega t + (b + d \, . \, l_{f,r}) \cos \omega t .$$

Thus, with sine and cosine inputs to the bridge, the galvanometer readings are proportional to $a + c \,.\, l_{f,r}$ and $b + d \,.\, l_{f,r}$, respectively. Knowing $l_{f,r}$ it is possible to find in-phase and out-of-phase amplitudes of the normal force and moment about C. We adopt the convention that normal force and moment are positive in the direction α increasing. Noting that the work done by the aerodynamic moment M_a over one cycle of the motion is

$$\int_0^{2\pi/\omega} M_a \,.\, \alpha_t \, dt = \int_0^{2\pi/\omega} (a \sin \omega t + b \cos \omega t)\alpha_0 \omega \cos \omega t \, dt = \pi b \alpha_0 \,,$$

the motion is damped when b is negative. The out-of-phase part of N (namely, d) indicates, by its magnitude and sign, the position of the out-of-phase centre of pressure.

Since α is small we may write $\sin \alpha \simeq \alpha$ and the inertia and weight terms can then be shown to lead to sting moments

$$M_{f,r} = (I_m - F \,.\, l \,.\, l_{f,r}) \sin \omega t - W(l - l_{f,r})\alpha_0 \sin \omega t \,.$$

Running a test with an in-phase bridge supply and the wind off will cause galvanometer deflections proportional to the amplitude of this expression and it was found, for the configuration tested, that the effect was a positive one in our convention. Thus a ready means existed for identification of this direction. It may be remarked that this was not an easy thing to discover from the circuit arrangements alone.

3.7. *The Bridge Circuits.*—The strain-gauges used for detection of the moments in the sting were Tinsley Type 20B, wire wound and of a nominal 125 ohms resistance. The active elements of these gauges were of small size, about $\frac{1}{8}$ in. wide and $\frac{5}{16}$ in. long, so that it was just possible to accommodate them on the sting after trimming their paper backings. The dummy gauges were of the usual Tinsley Type 6K (100 ohm) pattern of one inch length. These were mounted outside the tunnel and their insulation resistance to earth made as high as possible.

The electrical connections between active and dummy gauges consisted of 38 S.W.G. Eureka wire for the distance from the active gauges to a point just outside the wind tunnel, from where they were continued with standard plastic covered 20 S.W.G. copper wire. The small-gauge wire was necessary in order to make the connections inside the hollow model, the available space being a minimum. Great care was exercised to keep the insulation resistance to earth of the whole bridge circuit as high as possible and this eventually turned out to be about 60 megohms (*see* further remarks in Section 3.9).

Fig. 10 shows the wiring diagram for the front and rear bridge circuits and the galvanometer. The latter was a moving-coil reflecting instrument with an internal resistance of 50 ohms and a sensitivity of 130 scale divisions (millimetres) per micro-amp. In addition, the moving parts possessed sufficient inertia to keep the amplitudes of the harmonics in the bridge output down to acceptable values at all but the very lowest frequencies. Nevertheless, the response time was not so long as to make the taking of readings wasteful of tunnel running time. This was very convenient as the need for smoothing circuitry was eliminated.

3.8. *The Alternating Supply Voltage.*—It was essential to the successful operation of the system of measurement that a stable supply of alternating current should be available, its frequency being exactly that of the model displacement and its phase relationship to the latter being under control.

In Fig. 11, the circle of radius R represents an eccentric interruptor cam on the swash-plate driving spindle (*see* Fig. 6). The centre of the spindle is at C and e is the eccentricity of the cam. The light beam is of width D and, together with the photocell may be swung through a 90-deg arc about C (positions 1 and 2 in the sketch). With a light beam of constant depth and intensity the amount of light falling on the cathode is proportional to either I_1 or I_2 and, if coincidence of the lines AA and OC is taken to be the angular position at which the model is at zero incidence, then

$$I_1 = D - R + e \cos \omega t$$
$$I_2 = D - R + e \sin \omega t \,.$$

Thus the photocell provides sin ωt or cos ωt outputs, as required.

The construction of the motion-detecting equipment is illustrated in Fig. 12. The light source was a 24-watt, 12-volt single-filament bulb at the focal point of a suitable lens in the upper cylindrical unit, the lens being stopped down by a $\frac{1}{2}$ in. square aperture. Source and photocell were rigidly mounted on a backplate which could be rotated about a large disc attached to the drive shaft bearing cage (*see* Fig. 12). Also mounted on the disc was the light-beam zero stop which, once set, permitted the light beam to be swung through exactly 90 deg.

Power amplification for the photocell output was provided by the circuit shown in Fig. 13. The only significant source of phase variation with frequency was the coupling condensers necessary to split the photocell output before feeding it to the push-pull amplifier stage. This variation is shown in Fig. 14, from which it can be seen that, by correctly setting the phase of the light beam at a frequency of 10 c.p.s., the error introduced by ignoring the effect of the condensers is less than $\pm$ 1 deg from 5 c.p.s. upwards. Since it did not appear possible to set the equipment to better than $\pm$ 1 deg in phase angle (*see* Section 4, below), it was decided to neglect the condenser-produced variations and to zero-set the apparatus at 10 c.p.s.

The bridge input voltage was measured with a Cambridge Instrument Co. 5 mA vacuum thermo-junction, protected by a 2·2 kilo-ohm series resistor, and a sensitive millivoltmeter. Thus both A.C. and D.C. measurements could be made with the same instruments. Section 4.1 gives details of the calibrations.

In order to check that the amplifying circuitry did not introduce excessive harmonics into the bridge supply voltage, the amplifier and cathode follower stages were supplied with an input from an oscillator. Outputs from the oscillator and the cathode follower were displayed on a double-beam C.R.O. and visual matching showed the two outputs to be indistinguishable. This accuracy was all that was required.

3.9. *Insulation Resistance.*—As will be seen from the results to be discussed below, the oscillatory force and moment measurements showed a tendency to a scatter of more or less constant magnitude, irrespective of the magnitude of the moment being recorded. This constant scatter represents roughly 0·02 micro-amps through the galvanometer and, noting that either side of the strain-gauge bridge circuit is at + 40V above earth potential (*see* Fig. 13) it can readily be seen that this galvanometer current is accounted for by a 5 per cent change in insulation resistance, a plausible arrangement of these values being shown in Fig. 15.

From this rather over-simplified picture and also from other observations, such as a difference in D.C. and A.C. (as supplied by the circuit of Fig. 13) zeros, it was concluded that this insulation resistance defect accounted almost entirely for the observed experimental scatter. It could be largely eliminated by insulating the entire model mounting gear from earth and it is proposed to do this with future tests.

4. *Setting up the Light Beam.*—The light beam zero-stop was set to the correct position as follows : With the wind off, a large brass mass was attached to the sting in place of the model. This provided a large inertia term in the sting moment and negligible damping, *i.e.*, the moments detected by the strain-gauges were of the form $M_{f,r} = a \sin \omega t$. Let it now be supposed that the light beam is incorrectly phased by an amount ρ (*see* Fig. 11 for the direction of positive error). The bridge input voltage would then be $V = V_0 \cos(\omega t - \rho)$ in the ' out-of-phase ' position and bridge output would be proportional to $aV_0 \sin \rho$. If the galvanometer reading was zero, then ρ must have been zero. Reasonable sensitivity of adjustment was provided by making a large.

Thus, with some light-beam setting near to the correct one, the galvanometer reading was noted and, in addition, the effect of doubling the supply voltage amplitude, V_0, by means of the amplifier gain control. Any increase in the galvanometer reading on doubling V_0 indicated that ρ was not zero. The position of the light beam for which doubling of V_0 had no noticeable effect was taken as the correct out-of-phase setting. Locking of the light beam zero-stop then automatically located the in-phase position. Zero setting was accomplished to within one half

of one division galvanometer deflection. Since the in-phase reading was 45 divisions, accuracy of setting was to within about $\pm$ 1 deg. As stated previously, the zero was set at a frequency of 10 c.p.s.

4.1. *Calibration of Bridge Circuits.* The calibration of the strain-gauge bridge circuits was carried out as follows : Referring to Fig. 16, showing the sting lay-out, the single point load F produced moments

$$M_f = Fl'_f = KR_f$$

$$M_r = Fl'_r = KR_r$$

at the front and rear gauge positions respectively. R_f, R_r are the appropriate galvanometer deflections and K is the calibration factor (the latter was shown to be the same for each pair of gauges by applying a pure moment to the sting and finding that $R_f = R_r$). Plotting R_r and R_f against F enabled the ratios l'_f/K and l'_r/K to be found.

A single gauge covered a relatively large area of the sting and it was not possible to tell, therefore, exactly where its ' effective ' position for the measurement of strain was located. It seems reasonable to suppose that this position lies somewhere within the length of each individual gauge pair and, assuming that the two pairs are identical, it follows that $l'_r - l'_f$ equals the distance between the gauges (1·20 in. in the present instance). Knowing l'_f/K, l'_r/K and $l'_r - l'_f$ it was possible to find l'_f, l'_r and K. The accuracy of the assumptions was checked by finding K directly through application of a pure moment to the sting followed by calculation of $l'_r - l'_f$ and agreement was highly satisfactory. It was much easier to employ the single point load method of calibration when the model was mounted in the wind tunnel and checks on calibration could therefore be made frequently with reasonable ease.

Fig. 17 shows the results of a typical calibration run. The value of K used in the reduction of experimental results was $K = 0{\cdot}00275$ lb in./div., the (D.C.) supply voltage being 1·24mV as recorded on the vacuum thermo-junction meter. The calibration constant for any other D.C. supply voltage was therefore

$$K_{\text{D.C.}} = \frac{0{\cdot}00306}{\sqrt{(mV)}} \text{ lb. in./div.},$$

mV being the appropriate meter reading in millivolts.

When the supply voltage is of an alternating character, Section 3.5 shows that the D.C. part of the bridge output is one half of that which would arise with D.C. energisation. Since the thermo-junction gives millivoltmeter readings proportional to the heating effect of the supply voltage, the net effect is to decrease the A.C. sensitivity of the bridge outputs by a factor $\sqrt{2}$. Thus

$$K_{\text{A.C.}} = \frac{0{\cdot}00433}{\sqrt{(mV)}} \text{ lb in./div.}.$$

The distances of the effective strain-gauge pair positions from point C were

$$l_f = 0{\cdot}168 \text{ in.} : \; l_r = 1{\cdot}368 \text{ in.}.$$

4.2. *Inertia Measurements.*—A short series of experiments was conducted in which model inertia was measured and compared with values calculated from the apparatus constants and dimensions.

It has been shown in Section 3.6 that the combined inertia and weight forces produce moments at the gauge pair positions given by

$$M_{f,r} = (I_m - Fll_{f,r}) \sin \omega t - W(l - l_{f,r})\alpha_0 \sin \omega t .$$

Putting in the values

$$I_m = 0{\cdot}000124f^2 \text{ lb in.} \qquad l_f = 0{\cdot}168 \text{ in.}$$
$$F = 0{\cdot}00232f^2 \text{ lb} \qquad l_r = 1{\cdot}368 \text{ in.}$$
$$l = -0{\cdot}043 \text{ in.} \qquad W = 0{\cdot}036 \text{ lb}$$

and with $\alpha_o = 3$ deg we have

$$M_f = 0{\cdot}000126f^2 - 0{\cdot}0004 \text{ lb in.}$$
$$M_r = 0{\cdot}000138f^2 - 0{\cdot}0027 \text{ lb in.}$$

The frequency dependent part of these moments is shown plotted versus f^2 in Fig. 18, together with the experimental points. Agreement is seen to be quite satisfactory. The moments for the rear position appear to be slightly high, but this may be the effect of the inertia of the sting itself, which has not been accounted for in the calculations.

5. *Steady-State Measurements.*—A series of steady-state measurements of force and moment were made at three subsonic Mach numbers, 0·53, 0·67 and 0·78. The bridge circuits were supplied with D.C. at about 6V and model incidence was varied between $\pm$ 3 deg by rotation of the drive shaft. Incidence (to the tunnel centre-line) was measured on a scale round the periphery of the flexible coupling. The results are shown plotted in Figs. 19, 20 and 21. Unfortunately it was only possible to run tests at subsonic speeds in the $3\frac{1}{2}$ in. by 8 in. working-section, which was not entirely suited to the present equipment.

It can be seen that lift and moment are linear functions of incidence and also that zero incidence to tunnel centre-line does not correspond with zero angle of attack, as represented by zero lift. When normal force is zero, the symmetry of the model implies that moment should also be zero, but this is not in fact the case. All these effects are accounted for by support-shroud interference which causes the stream to be slightly curved in the vicinity of the model. It seems reasonable to suppose that true lift and moment at an angle of attack of 3 deg can be deduced from the slopes of the curves vs. incidence as these are linear to a good approximation. Values deduced in this way are shown plotted on Figs. 23, 24 and 26, for comparison with the results of oscillatory measurements.

Support interference will largely disappear when tests are conducted at supersonic Mach numbers.

5.1. *Oscillatory Forces and Moments. In-Phase Measurements.*—Experimental values of in-phase forces and moments were obtained at a variety of frequencies between 4 c.p.s. and 16 c.p.s. and at eight subsonic Mach numbers from 0·41 to 0·85. Reynolds number, based on model length, varied between $0{\cdot}75 \times 10^6$ to $1{\cdot}25 \times 10^6$. The model was oscillated in a pitching mode about its mid-point, the amplitude being 3 deg.

The moments experienced in the sting at the gauge positions (in lb in.) are shown plotted against frequency for the various Mach numbers in Figs. 22 to 29, inclusive.

A comparison of the zero-frequency sting moments with those measured while the model was oscillating indicates that variation of in-phase aerodynamic force and moment with frequency is less than the experimental scatter. Theory (Ref. 5), shows that in-phase frequency effects are proportional to k^2, and the experimental results are at least consistent with so small a variation (N.B.—k is the usual reduced frequency parameter, based on model length).

The amplitudes of aerodynamic normal-force coefficient and pitching-moment coefficient about the first strain-gauge pair measuring position (1·918 in. behind the nose) have been calculated, based on maximum model cross-section and model length. They are shown plotted against Mach number in Fig. 30. Normal-force coefficient shows a tendency to rise as Mach number

increases. The pitching moment coefficient, however, appears to be roughly constant for all Mach numbers, within the limits of experimental error. The normal-force coefficient at $M = 0{\cdot}41$ appears to be rather low, but for the reasons explained in Section 3.9, the experimental scatter was of roughly constant magnitude and hence its effect was felt most when the forces to be measured were small. With this in mind the curve for C_n vs. M drawn in Fig. 30 probably represents a reasonable estimate of the true state of affairs.

Also shown on Fig. 30 are theoretical values for C_n and C_m, calculated from first-order slender-body theory. Such a theory is strictly invalid for the configuration tested for two reasons. Firstly, it applies only to bodies pointed at both ends and secondly it takes no account of sharp corners in their meridian profiles. The first objection is probably not a serious one here, as sting afterbody effects on the test model are in all probability small, but the second deficiency in the theory is almost certainly very important. A corner such as the cone-cylinder junction on the test model may promote at least a local separation of the boundary layer in its vicinity, and in order to investigate such possible effects the flow past the oscillating model was photographed by a high-speed camera, using the Schlieren technique for flow visualisation. The subsonic Mach number and smallness of the model made detailed observation extremely difficult, but it was just possible to distinguish the boundary layer after enlargement of the films. There was no evidence of boundary-layer separation anywhere on the model and in addition there was no observable difference between the oscillatory and steady flows (this may be taken as some confirmation of the equality of sting moments in the two cases). The thickening of the boundary layer which was observed downstream of the cone-cylinder junction would give rise to a potential flow past a body whose cross-section continued to increase and this may account, at least qualitatively, for the observed difference between the (rather crude) theory and the actual measurements.

Schlieren observation showed that the tunnel choked at $M = 0{\cdot}847$ in the region of the model supports. No shock phenomena were apparent on the model at this Mach number.

5.2. *Oscillatory Forces and Moments. Out-of-Phase Tests.*—Theory indicates that the out-of-phase force and moment coefficients are of the same order of magnitude as the reduced frequency parameter, k. Thus it was apparently necessary to measure phase angles of the order of 2 deg or 3 deg, or their equivalent in terms of out-of-phase amplitudes. These quantities are of comparable order to the accuracy of the measuring equipment and the previously experienced experimental error, so that the subject of out-of-phase tests was approached with two objects in mind. Firstly, the tests may have shown up any radical departures from the anticipated values and secondly they would give some further indications of the accuracy of the experimental set-up.

A series of tests covering the range of Mach number from $0{\cdot}4$ to $0{\cdot}85$ and frequency from 6 to 16 c.p.s. consistently gave values of sting moments at both front and rear positions about $-0{\cdot}002$ lb. in. in magnitude. This is generally consistent with the estimate of a phase angle of the order of one or two degrees which is suggested by theory. Furthermore, the sign suggested that the motion was positively damped. It was, of course, not possible to obtain anything more accurate than these estimates (for the configuration tested) for the reasons stated previously.

The magnitude of the measured moments tended to confirm the accuracy of the light-beam phasing since the front and rear gauge values would be widely different, as in the in-phase case, if the galvanometer had simply been recording a fraction of these in-phase values due to incorrect light-beam setting. It may be safely said that the out-of-phase effects and accuracy of the equipment are of the same order of magnitude, as theory would suggest.

5.3. *Concluding Remarks.*—The preliminary tests with the apparatus described above have been encouraging and rectification of the insulation resistance trouble mentioned in Section 3.9, should permit accurate measurement of sting moments down to $0{\cdot}01$ lb in. at least. This will enable experimental values of forces and moments on, say, a simple cone to be compared with theoretical estimates. The equipment will probably be most useful for direct measurements of the characteristics of wing-body combinations oscillating in a supersonic stream.

Acknowledgements.—This paper is based on the experimental part of the work carried out by the author between 1952 and 1955 for the degree of Ph.D. in the faculty of Aeronautical Engineering, University of London. He would like to express his gratitude to Dr. L. G. Whitehead for his help and encouragement throughout, to the late Prof. N. A. V. Piercy for suggesting the problem, to Prof. A. D. Young for the interest he has shown in the work and to Mr. A. Chinneck of the N.P.L. for his kind assistance with the high-speed photography. The author is also indebted to the Department of Scientific and Industrial Research for the provision of a maintenance grant over the period during which the work was carried out.

REFERENCES

No.	*Author*	*Title, etc.*
1	J. B. Bratt and A. Chinneck ..	Measurements of mid-chord pitching-moment derivatives at high speeds. R. & M. 2680. June, 1947.
2	N. A. V. Piercy	*Aerodynamics.* 2nd edition. English Universities Press. 1947.
3	W. J. Duncan	*The Principles of Control and Stability of Aircraft.* Cambridge University Press. 1952.
4	J. Valensi	A review of the techniques of measuring oscillatory aerodynamic forces and moments on models oscillating in wind tunnels in use on the continent. A.G.A.R.D. Publ. (AG 15/P6). pp. 14 to 49. May, 1954.
5	J. F. Clarke	Thesis. Queen Mary College, University of London. June, 1956.

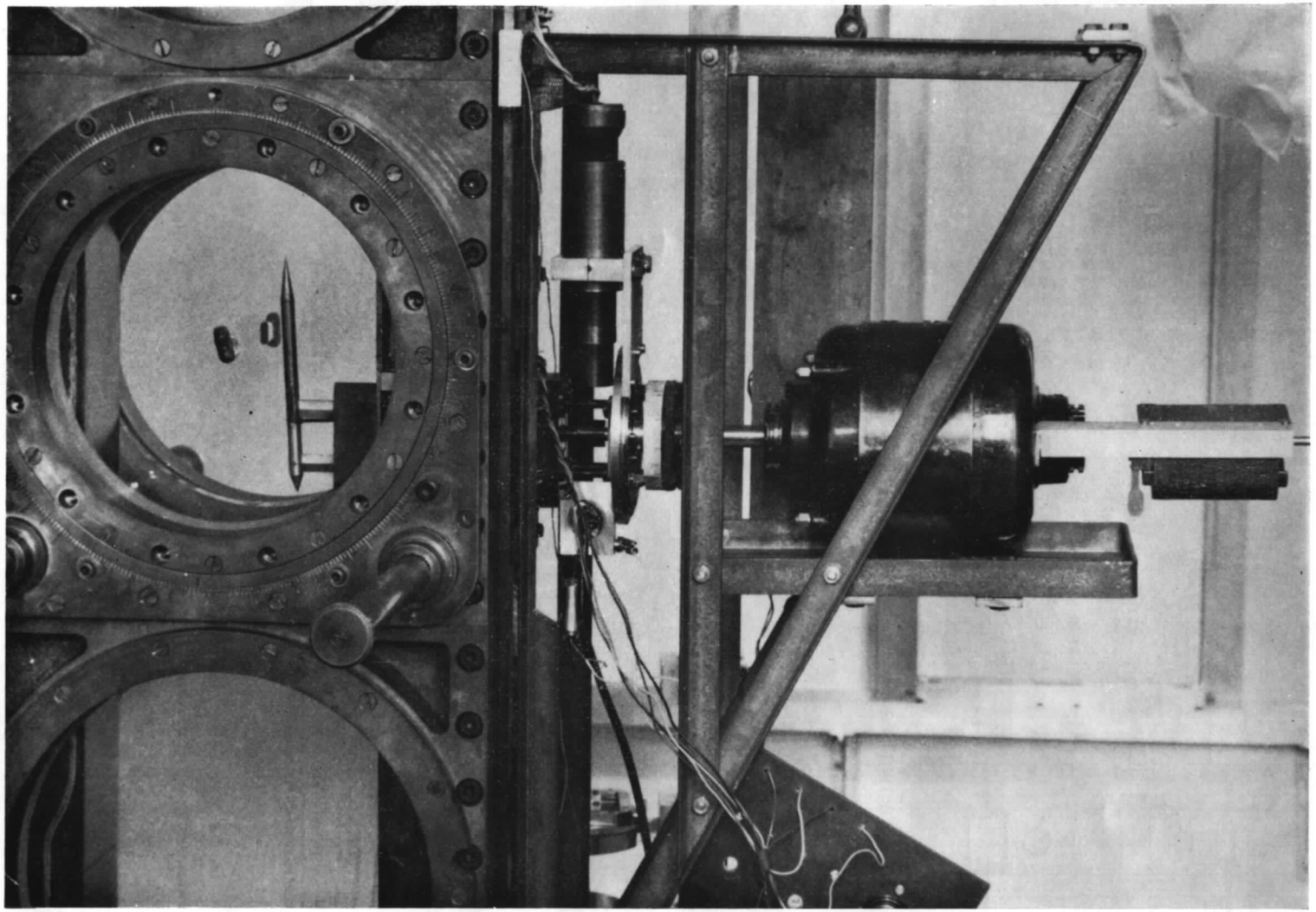

FIG. 1. General view of the apparatus.

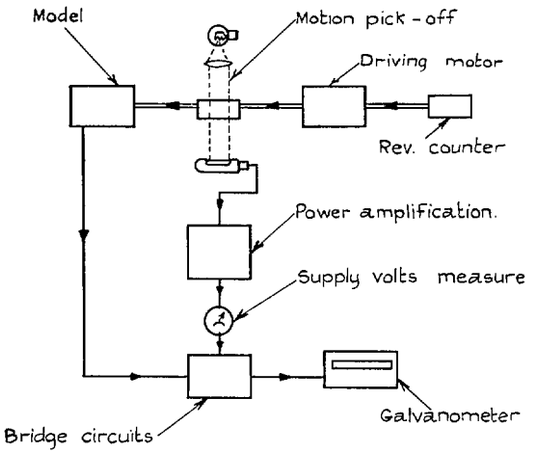

FIG. 2. Block diagram of apparatus.

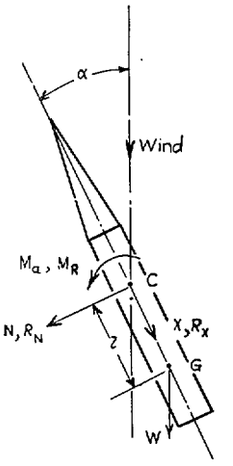

FIG. 4a. Actual forces.

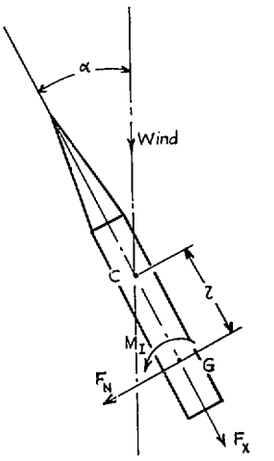

FIG. 4b. Effective forces.

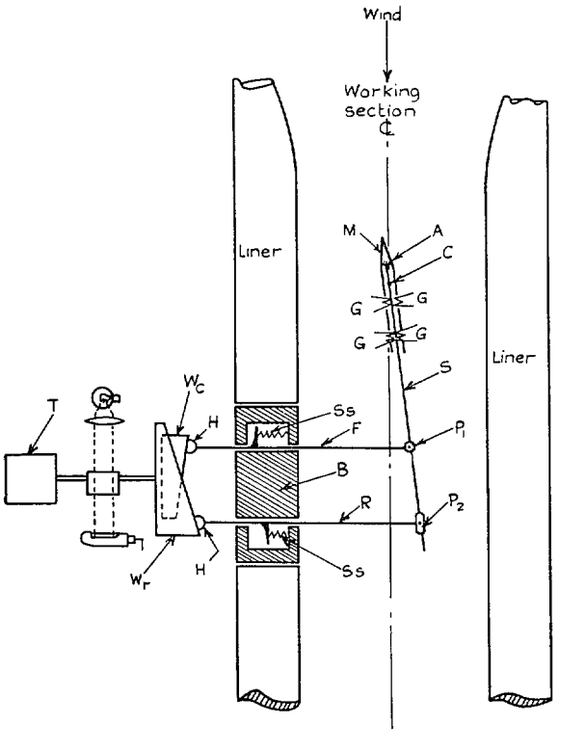

FIG. 3. The forcing gear (Diagrammatic).

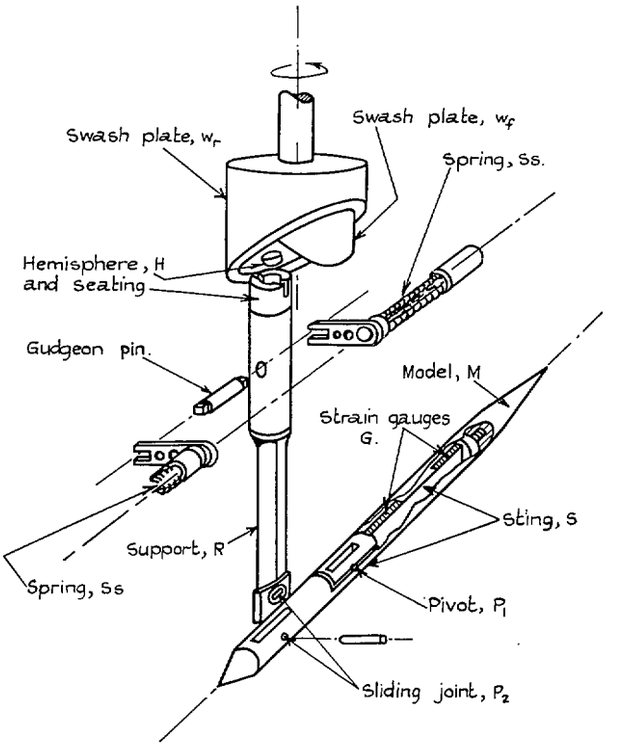

FIG. 5. Exploded view of drive and supports, etc. (Front support omitted for clarity).

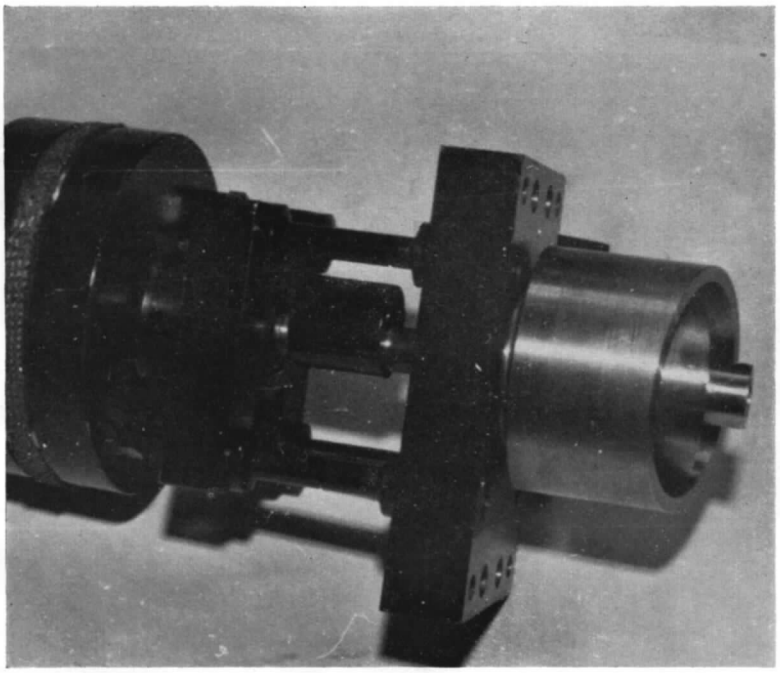

FIG. 6. The driving assembly (Swash plates, eccentric interruptor and flexible coupling).

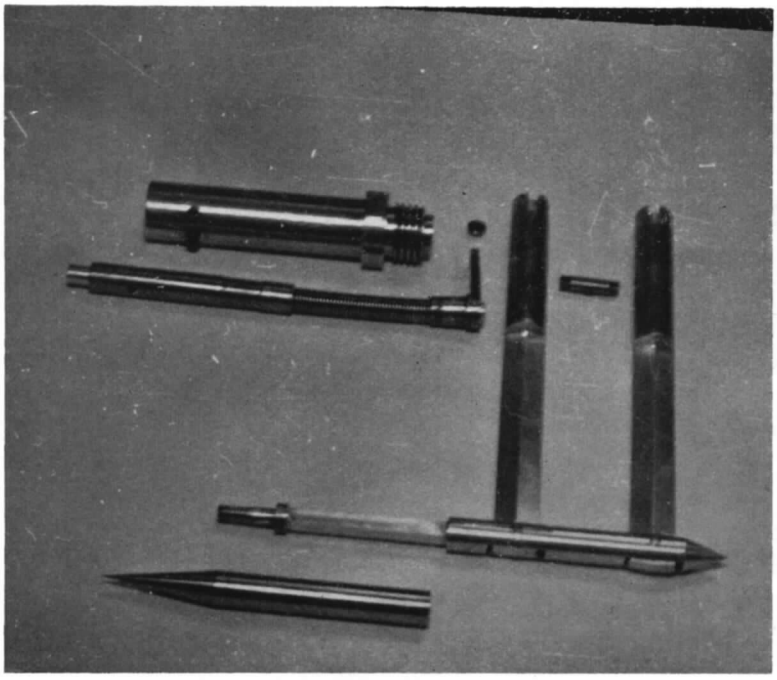

FIG. 7. Components of the forcing gear (Model, sting and supports, gudgeon pin, spring assembly and tube, hemisphere).

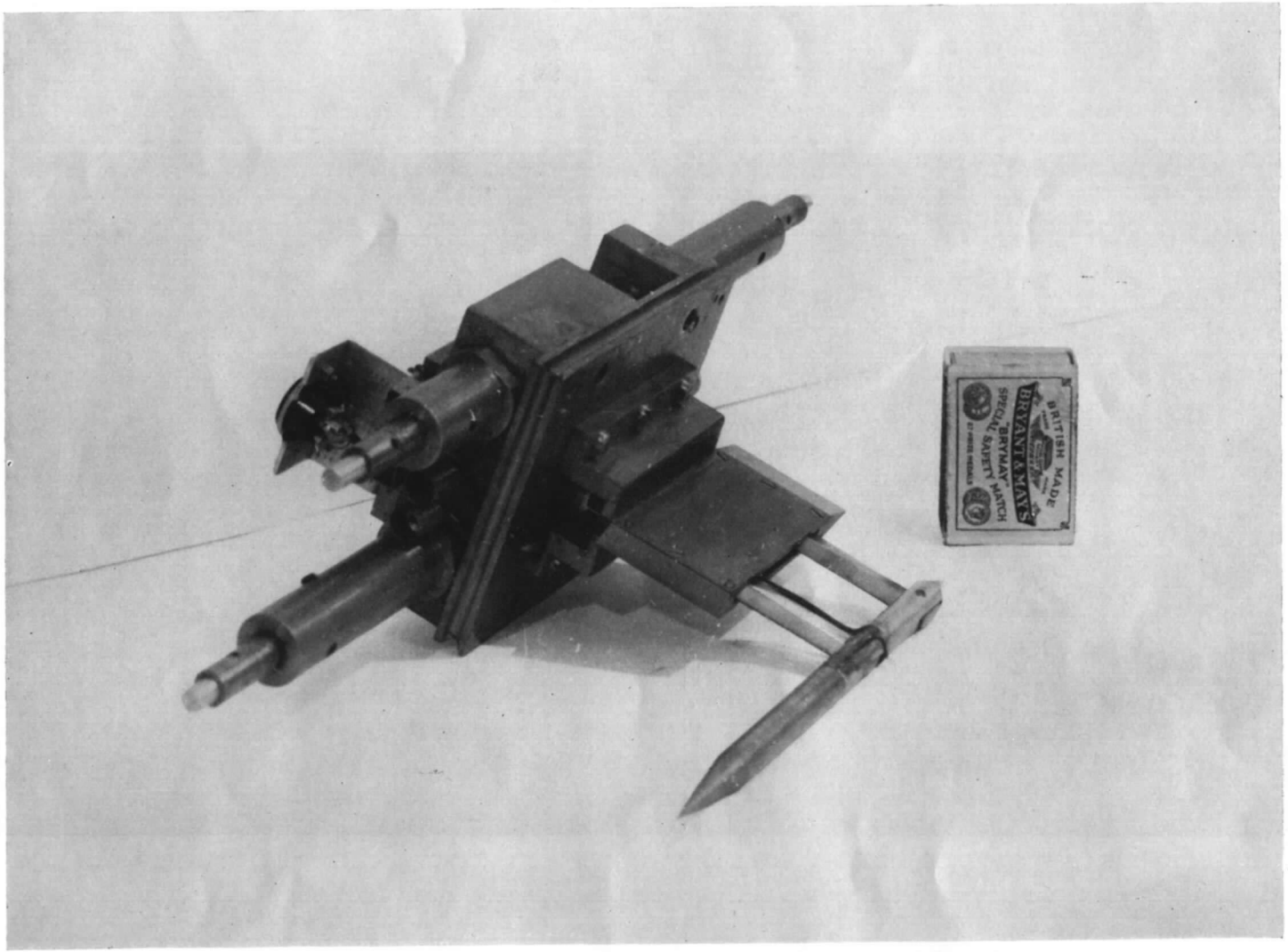

FIG. 8. Complete model and support assembly.

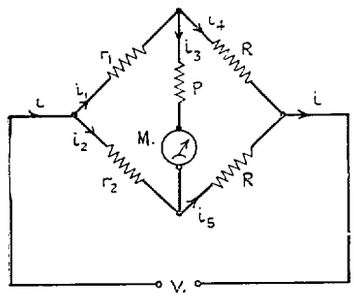

V Supply volts.
r_1, r_2 Active strain gauge resistance.
R Dummy strain gauge resistance.
M Galvanometer
P Internal resistance of galvanometer.
i_n Current, amps.
$r_1 = r + \delta r$
$r_2 = r - \delta r$

FIG. 9. Wheatstone bridge.

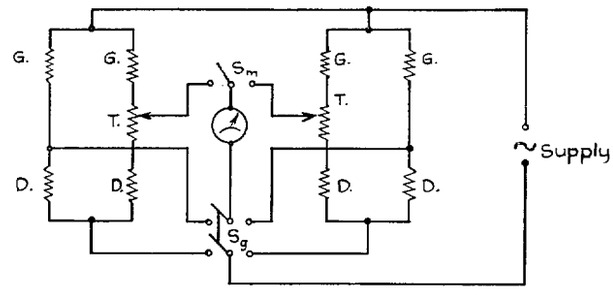

G Active gauges, 125 Ω.
D Dummy gauges, 100 Ω
T Trimmer resistances, 1 Ω
M Galvanometer
S_m Galvo. Isolating switch
S_g Ganged change-over switch.

FIG. 10. Bridge circuits.

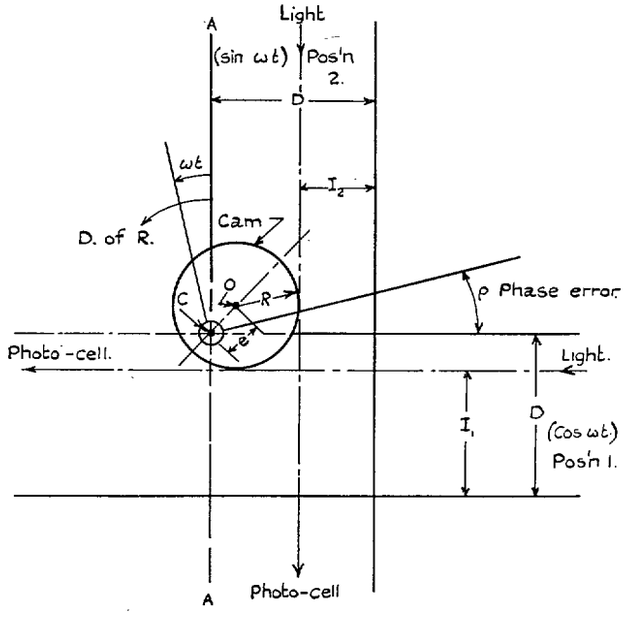

FIG. 11. Arrangement of light beam and eccentric interruptor cam.

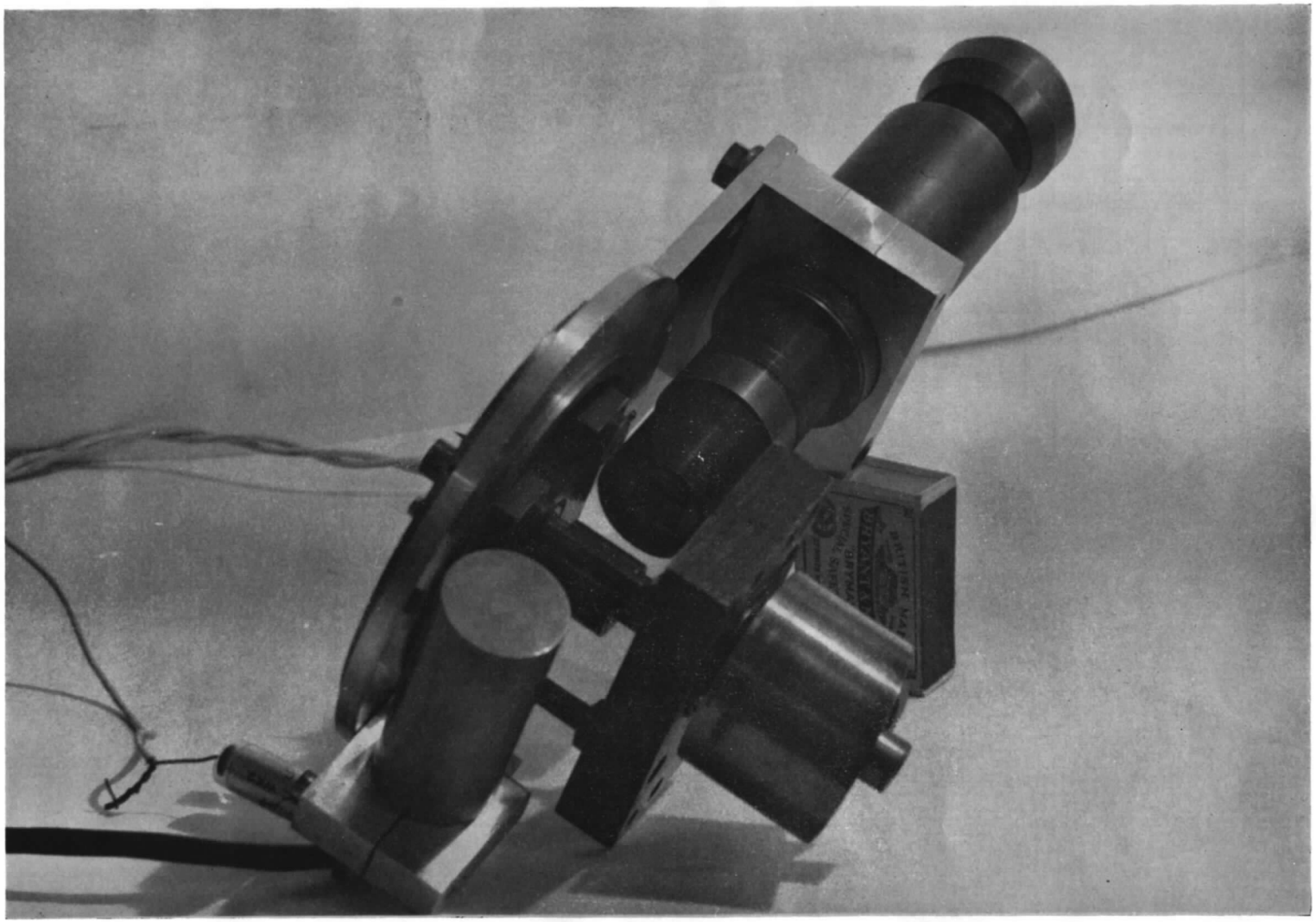

FIG. 12. Driving gear and photo-cell assembly.

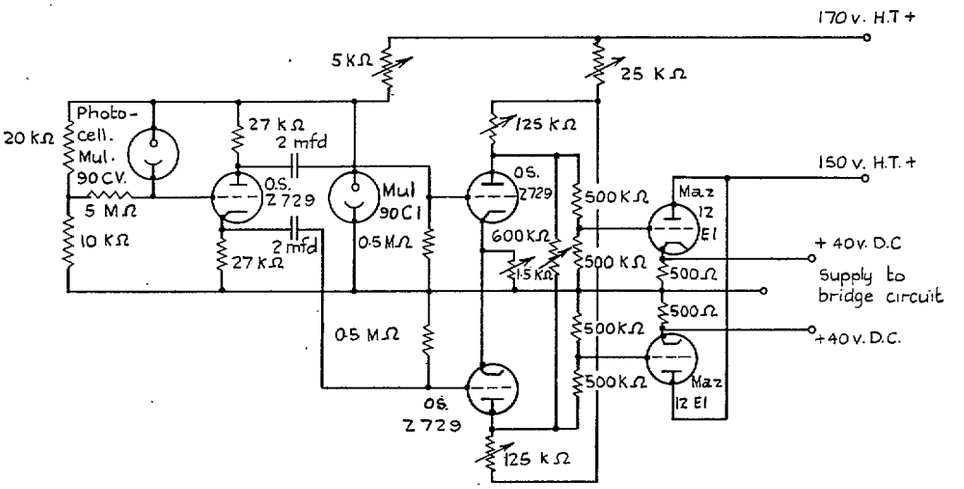

FIG. 13. Photo-cell and amplifying circuit.

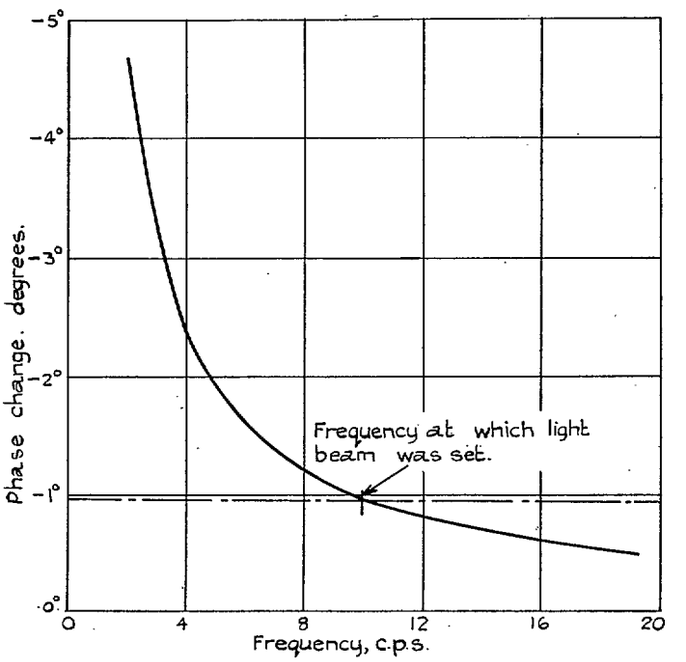

FIG. 14. Electrical phase change vs. frequency.

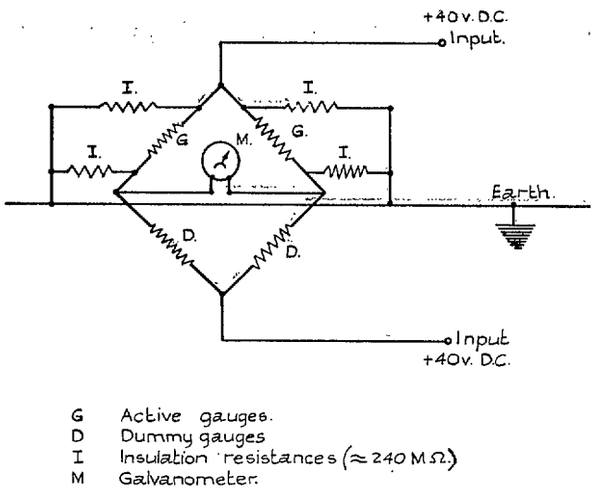

FIG. 15. Insulation resistance (Assumed).

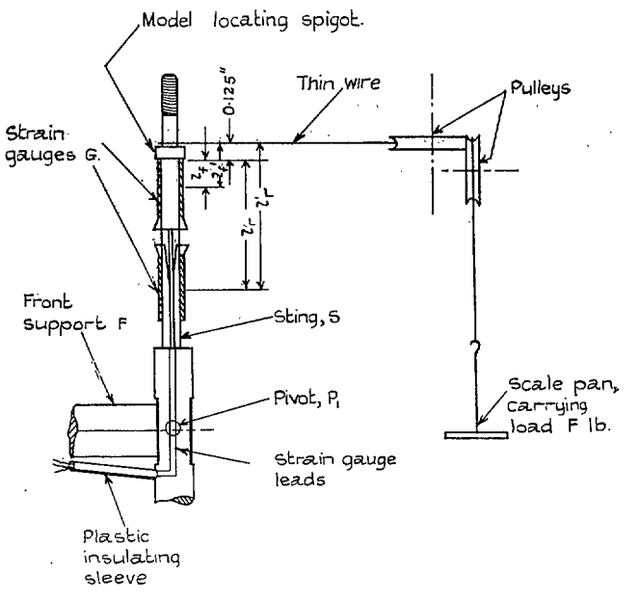

FIG. 16. Strain-gauge calibration.

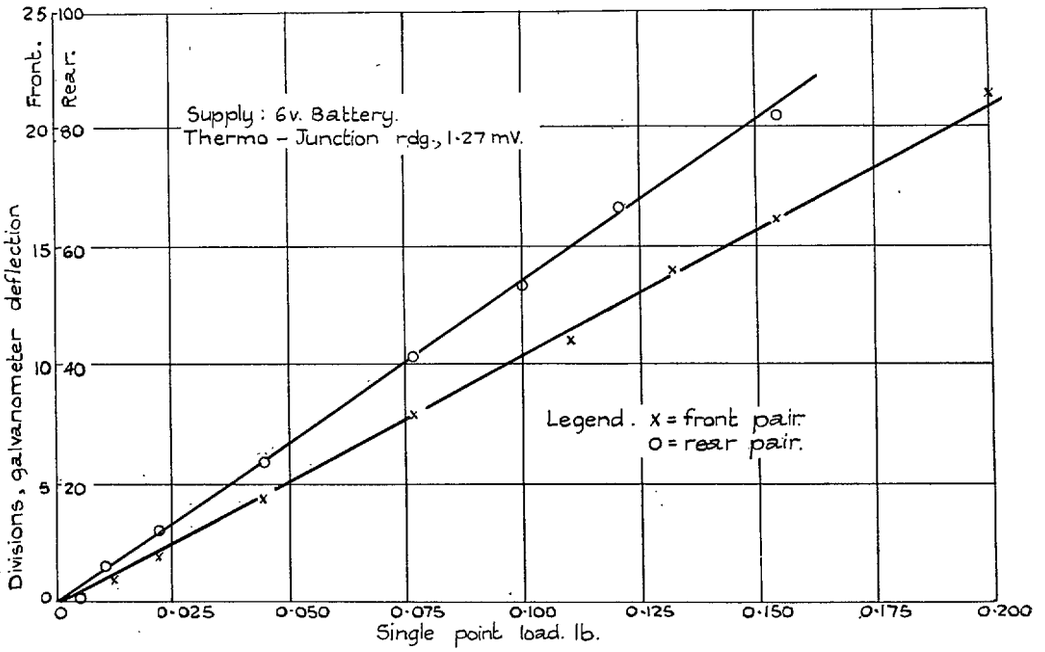

FIG. 17. Calibration of the measuring equipment.

(78669)

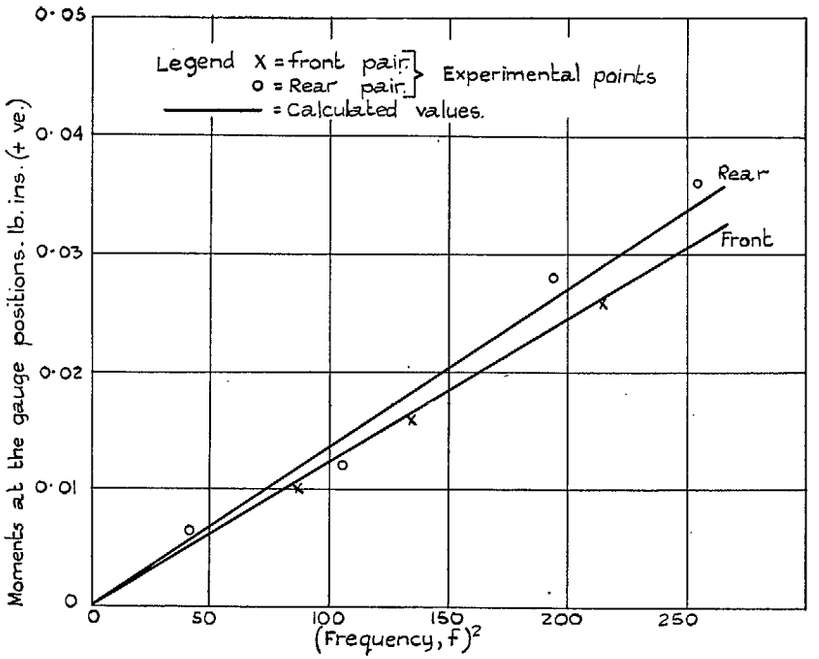

FIG. 18. Moments at the gauge positions due to inertia effects (wind off) vs. (frequency)².

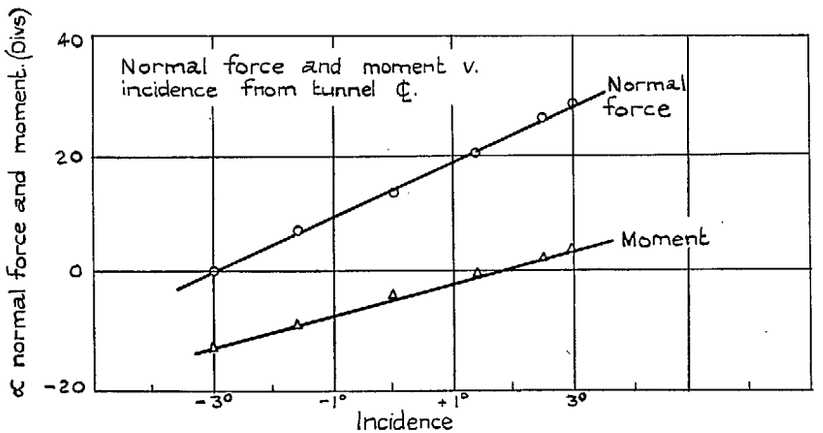

FIG. 19. Steady-state measurements. $M = 0{\cdot}53$. $mV = 1{\cdot}30$.

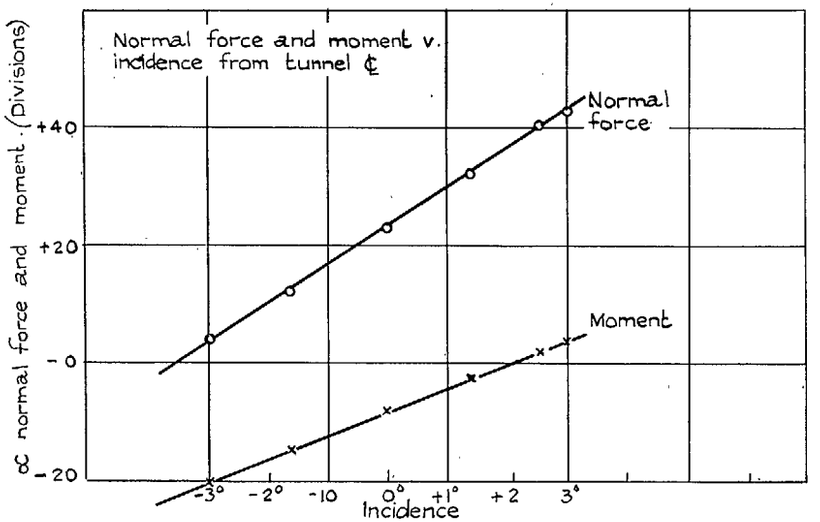

FIG. 20. Steady-state measurements. $M = 0{\cdot}67$. $mV = 1{\cdot}30$.

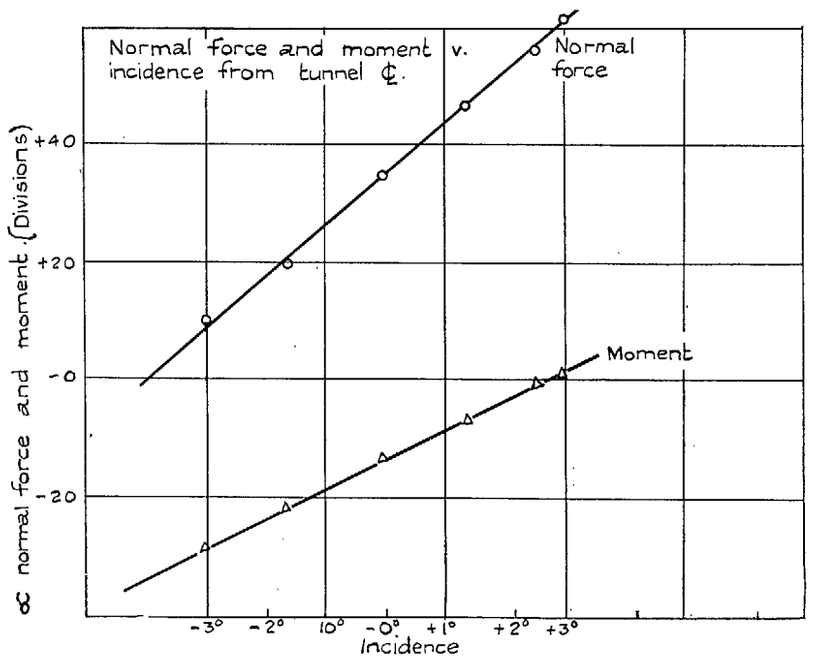

FIG. 21. Steady-state measurements. $M = 0{\cdot}78$. $mV = 1{\cdot}30$.

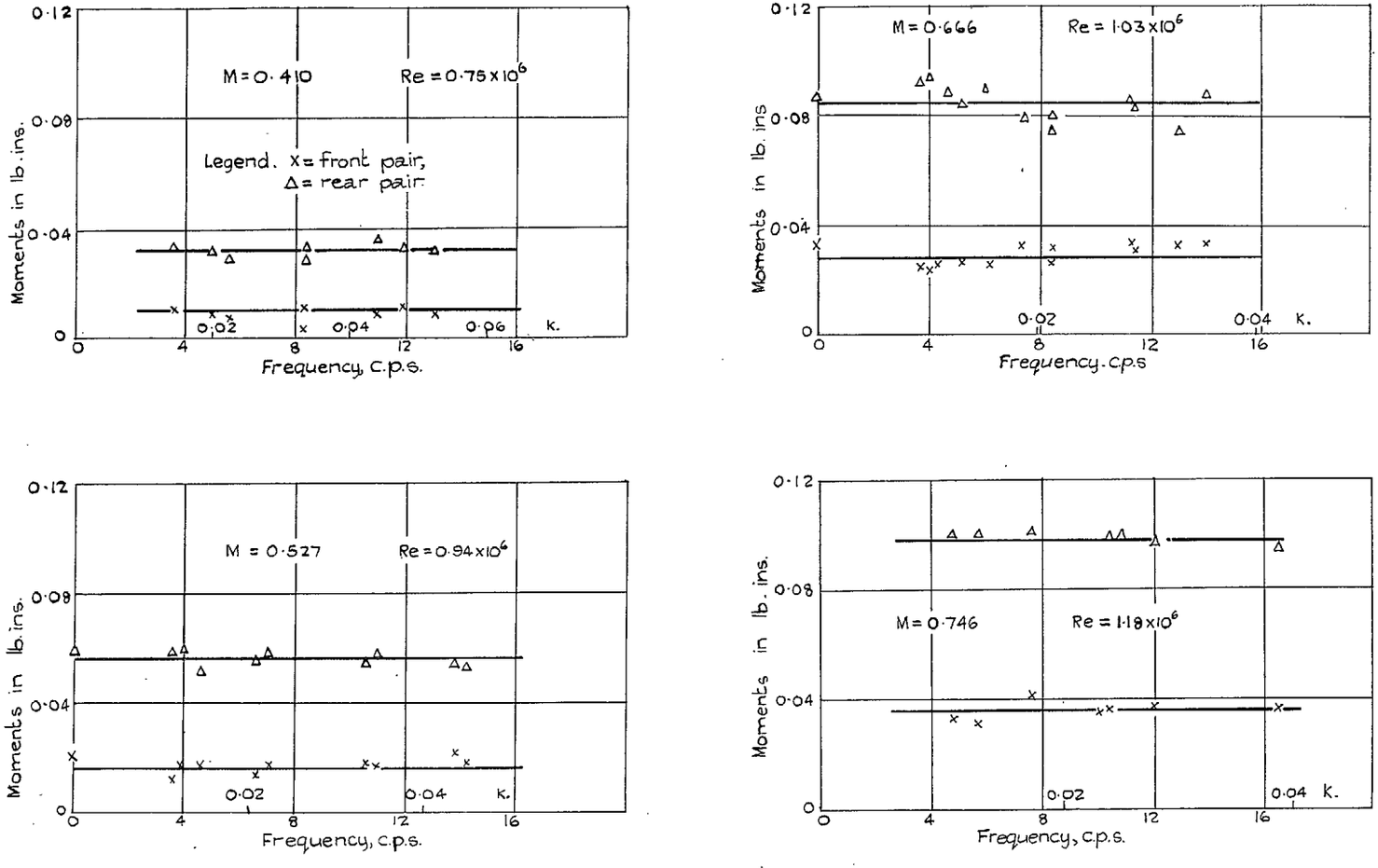

FIGS. 22 to 25. In-phase moments measured at the gauge positions (lb in.) vs. frequency (c.p.s.) at various Mach numbers.

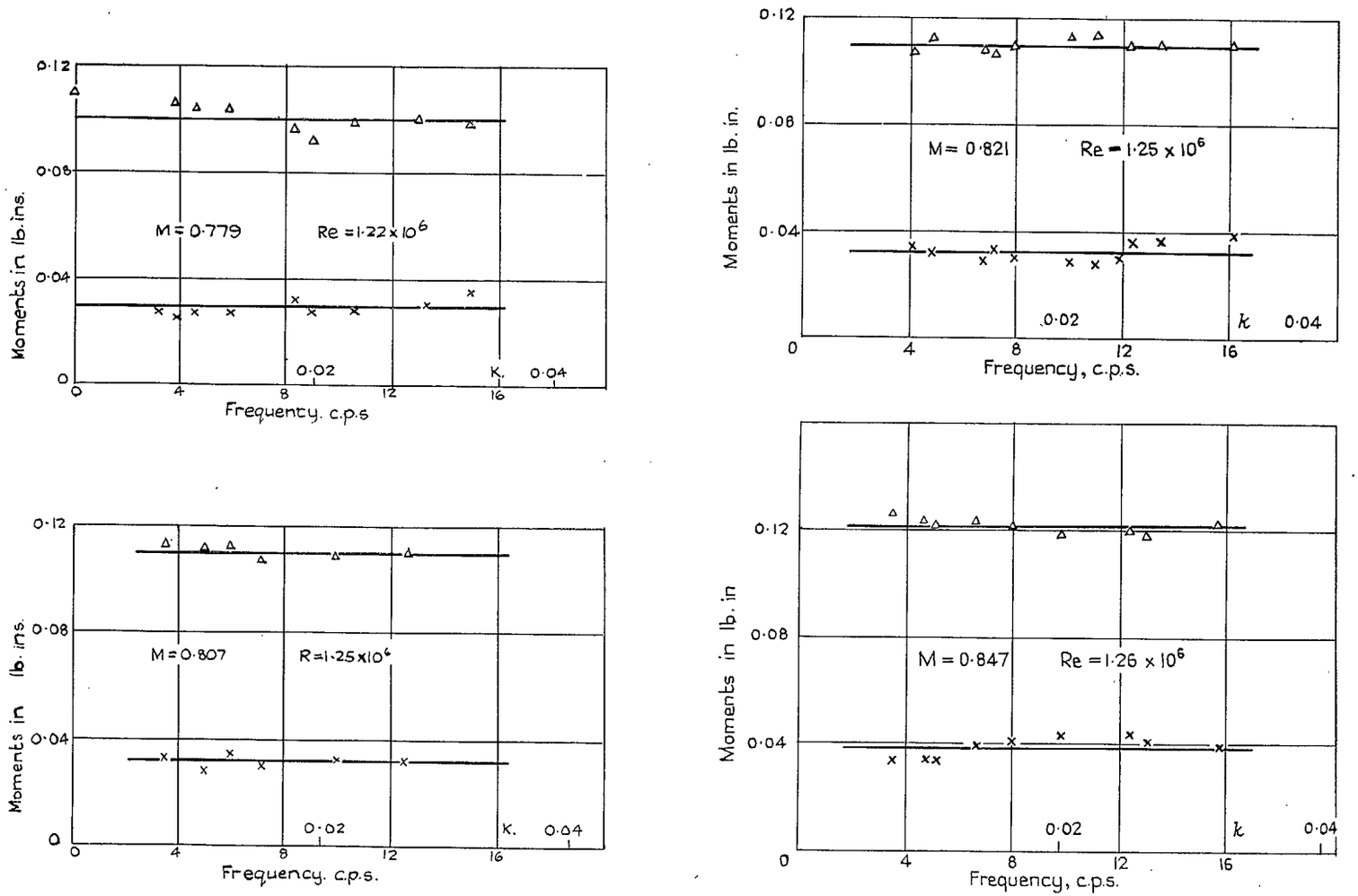

FIGS. 26 to 29. In-phase moments measured at the gauge positions (lb in.) vs. frequency (c.p.s.) at various Mach numbers,

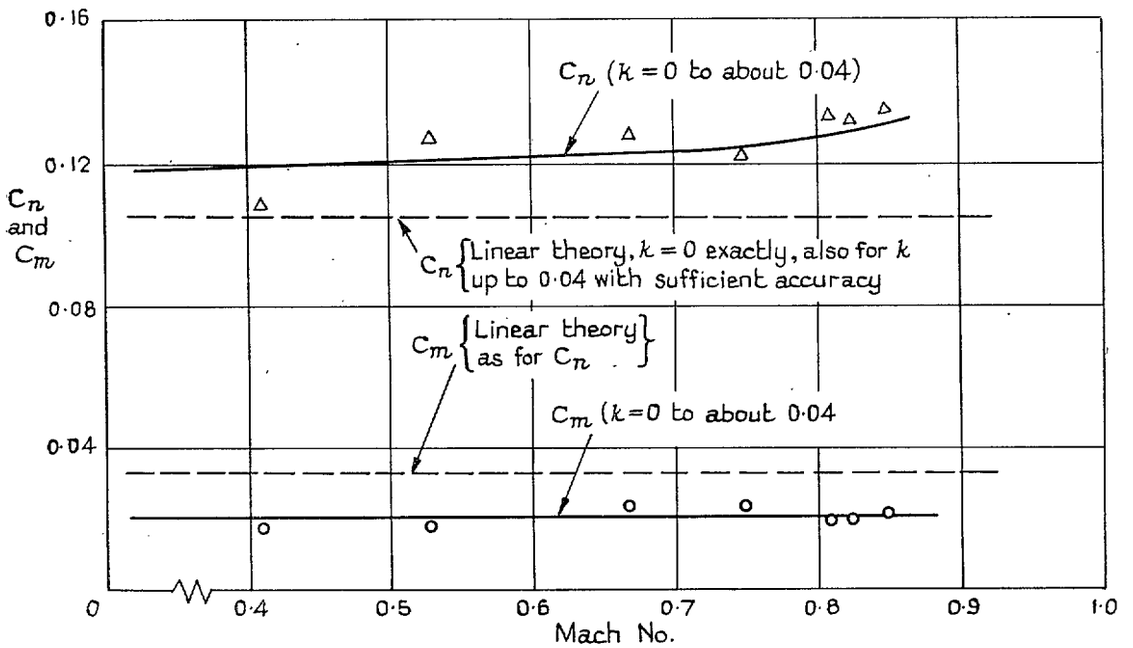

FIG. 30. In-phase normal-force and pitching-moment coefficients vs. Mach-number pitching motion ; amplitude 3 deg.

(78669) Wt. 3523/8210 K7 8/60 Hw. PRINTED IN ENGLAND

Publications of the Aeronautical Research Council

ANNUAL TECHNICAL REPORTS OF THE AERONAUTICAL RESEARCH COUNCIL (BOUND VOLUMES)

1939 Vol. I. Aerodynamics General, Performance, Airscrews, Engines. 50*s.* (52*s.*)
Vol. II. Stability and Control, Flutter and Vibration, Instruments, Structures, Seaplanes, etc. 63*s.* (65*s.*)

1940 Aero and Hydrodynamics, Aerofoils, Airscrews, Engines, Flutter, Icing, Stability and Control, Structures, and a miscellaneous section. 50*s.* (52*s.*)

1941 Aero and Hydrodynamics, Aerofoils, Airscrews, Engines, Flutter, Stability and Control, Structures. 63*s.* (65*s.* 3*d.*)

1942 Vol. I. Aero and Hydrodynamics, Aerofoils, Airscrews, Engines. 75*s.* (77*s.* 3*d.*)
Vol. II. Noise, Parachutes, Stability and Control, Structures, Vibration, Wind Tunnels. 47*s.* 6*d.* (49*s.* 3*d.*)

1943 Vol. I. Aerodynamics, Aerofoils, Airscrews. 80*s.* (82*s.*)
Vol. II. Engines, Flutter, Materials, Parachutes, Performance, Stability and Control, Structures. 90*s.* (92*s.* 3*d.*)

1944 Vol. I. Aero and Hydrodynamics, Aerofoils, Aircraft, Airscrews, Controls. 84*s.* (86*s.* 6*d.*)
Vol. II. Flutter and Vibration, Materials, Miscellaneous, Navigation, Parachutes, Performance, Plates and Panels, Stability, Structures, Test Equipment, Wind Tunnels. 84*s.* (86*s.* 6*d.*)

1945 Vol. I. Aero and Hydrodynamics, Aerofoils. 130*s.* (133*s.*)
Vol. II. Aircraft, Airscrews, Controls. 130*s.* (133*s.*)
Vol. III. Flutter and Vibration, Instruments, Miscellaneous, Parachutes, Plates and Panels, Propulsion. 130*s.* (132*s.* 9*d.*)
Vol. IV. Stability, Structures, Wind Tunnels, Wind Tunnel Technique. 130*s.* (132*s.* 9*d.*)

1947 Vol. I. Aerodynamics, Aerofoils, Aircraft. 168*s.* (171*s.* 3*d.*)

Annual Reports of the Aeronautical Research Council—

1939–48 3*s.* (3*s.* 5*d.*) 1949–54 5*s.* (5*s.* 5*d.*)

Index to all Reports and Memoranda published in the Annual Technical Reports, and separately—

April, 1950 - - - - R. & M. 2600 6*s.* (6*s.* 2*d.*)

Published Reports and Memoranda of the Aeronautical Research Council—

Between Nos. 2351–2449	R. & M. No. 2450	2*s.* (2*s.* 2*d.*)
Between Nos. 2451–2549	R. & M. No. 2550	2*s.* 6*d.* (2*s.* 8*d.*)
Between Nos. 2551–2649	R. & M. No. 2650	2*s.* 6*d.* (2*s.* 8*d.*)
Between Nos. 2651–2749	R. & M. No. 2750	2*s.* 6*d.* (2*s.* 8*d.*)
Between Nos. 2751–2849	R. & M. No. 2850	2*s.* 6*d.* (2*s.* 8*d.*)
Between Nos. 2851–2949	R. & M. No. 2950	3*s.* (3*s.* 2*d.*)

Prices in brackets include postage

HER MAJESTY'S STATIONERY OFFICE

York House, Kingsway, London W.C.2; 423 Oxford Street, London W.1; 13a Castle Street, Edinburgh 2; 39 King Street, Manchester 2; 2 Edmund Street, Birmingham 3; 109 St. Mary Street, Cardiff; 50 Fairfax Street, Bristol 1; 80 Chichester Street, Belfast 1, *or through any bookseller.*

S.O. Code No. 23-3170